Norrin stimulates cell proliferation in the superficial retinal vascular plexus and is pivotal for the recruitment of mural cells

Zuercher, Jurian ; Fritzsche, Martin ; Feil, Silke ; Mohn, Lucas ; Berger, Wolfgang

Abstract: Mutations in Norrin, the ligand of a receptor complex consisting of FZD4, LRP5 and TSPAN12, cause severe developmental blood vessel defects in the retina and progressive loss of the vascular system in the inner ear, which lead to congenital blindness and progressive hearing loss, respectively. We now examined molecular pathways involved in developmental retinal angiogenesis in a mouse model for Norrie disease. Comparison of morphometric parameters of the superficial retinal vascular plexus (SRVP), including the number of filopodia, vascular density and number of branch points together with inhibition of Notch signaling by using DAPT, suggest no direct link between Norrin and Notch signaling during formation of the SRVP. We noticed extensive vessel crossing within the SRVP, which might be a loss of Wnt- and MAP kinase-characteristic feature. In addition, endomucin was identified as a marker for central filopodia, which were aligned in a thorn-like fashion at P9 in Norrin knockout (Ndp(y/-)) mice. We also observed elevated mural cell coverage in the SRVP of Ndp(y/-) mice and explain it by an altered expression of PDGF and its receptor (PDGFR). In vivo cell proliferation assays revealed a reduced proliferation rate of isolectin B4-positive cells in the SRVP from Ndp(y/-) mice at postnatal day 6 and a decreased mitogenic activity of mutant compared with the wild-type Norrin. Our results suggest that the delayed outgrowth of the SRVP and decreased angiogenic sprouting in Ndp(y/-) mice are direct effects of the reduced proliferation of endothelial cells from the SRVP.

DOI: https://doi.org/10.1093/hmg/dds087

Norrin stimulates cell proliferation in the superficial retinal vascular plexus and is pivotal for the recruitment of mural cells

[#]Jurian Zuercher[1,2], [#]Martin Fritzsche[1], Silke Feil[1], Lucas Mohn[1,2], Wolfgang Berger[1,2,3,*]

[1]Institute of Medical Molecular Genetics, University of Zurich, Zurich, Switzerland
[2]Neuroscience Center Zurich (ZNZ), University of Zurich, Zurich, Switzerland
[3]Center for Integrative Human Physiology (ZIHP), University of Zurich, Zurich, Switzerland

[#]These two authors contributed equally

[*]To whom correspondence should be addressed at: Schorenstrasse 16, CH-8603 Schwerzenbach, phone: + 41 44 655 7031, fax: + 41 44 655 7213, email: berger@medmolgen.uzh.ch

Manuscript accepted from *Human Molecular Genetics*, February 28th 2012.

Abstract

Mutations in Norrin, the ligand of a receptor complex consisting of FZD4, LRP5 and TSPAN12, cause severe developmental blood vessel defects in the retina and progressive loss of the vascular system in the inner ear, which lead to congenital blindness and progressive hearing loss, respectively. We now examined molecular pathways involved in developmental retinal angiogenesis in a mouse model for Norrie disease. Comparison of morphometric parameters of the superficial retinal vascular plexus (SRVP), including the number of filopodia, vascular density and number of branch points together with inhibition of Notch signaling by using DAPT, suggest no direct link between Norrin and Notch signaling during formation of the SRVP. We noticed extensive vessel crossing within the SRVP, which might be a loss of Wnt- and MAP kinase-characteristic feature. In addition, endomucin was identified as a marker for central filopodia, which were aligned in a thorn-like fashion at P9 in Norrin knockout ($Ndp^{y/-}$) mice. We also observed elevated mural cell (MC) coverage in the SRVP of $Ndp^{y/-}$ mice and explain it by an altered expression of *PDGFβ* and its receptor (*PDGFRβ*). *In vivo* cell proliferation assays revealed a reduced proliferation rate of isolectinB4 positive cells in the SRVP from $Ndp^{y/-}$ mice at postnatal day 6 and a decreased mitogenic activity of mutant compared to the wildtype Norrin. Our results suggest that the delayed outgrowth of the SRVP and decreased angiogenic sprouting in $Ndp^{y/-}$ mice are direct effects of the reduced proliferation of endothelial cells from the SRVP.

Introduction

Mutations in the human *NDP* (*Norrie disease pseudoglioma*) gene, encoding Norrin, cause congenital blindness, progressive deafness and mental retardation, a triad of symptoms characteristic for Norrie

Disease (ND) (1-5). Alternatively, mutations in *NDP* can exclusively lead to ocular symptoms in X-linked exudative vireoretinopathy (EVR)(6), Coats' disease and retinopathy of prematurity (7,8). EVR is also caused by mutations in Frizzled-4 (*FZD4*, FZD4), low-density lipoprotein receptor-related protein 5 (*LRP5*, LRP5) or Tetraspanin-12 (*TSPAN12*, TSPAN12) (9-11). Recessive mutations in *Lrp5* may also cause osteoporosis pseudoglioma syndrome (OPPG), which manifests with low bone mass in addition to the ocular phenotype in patients (OMIM: #259770). It has been shown *in vitro* that Norrin is a ligand for the canonical Wnt signaling receptor complex consisting of FZD4, LRP5 and TSPAN12 (12,13). Furthermore, the outgrowth of the superficial retinal vascular plexus (SRVP) from $Ndp^{y/-}$, $Fzd4^{-/-}$, $Lrp5^{-/-}$ and $Tspan12^{-/-}$ is delayed and incomplete and all of these knockout mice lack the deep and intermediate retinal vascular plexuses (12-16). We generated and examined a Norrin knockout mouse model ($Ndp^{y/-}$) that resembles the human Norrie disease phenotype with respect to blindness and hearing loss (4,14,17). Hyaloid vessels do not completely regress in $Ndp^{y/-}$, $Fzd4^{-/-}$, $Lrp5^{-/-}$ and $Tspan12^{-/-}$ knockout mice (12-14,16). Retinal vascular hemorrhage and exudation from retinal blood vessels in *Ndp* knockout mice ($Ndp^{y/-}$) are characteristic features. We previously demonstrated that expression of the plasmalemma vesicle-associated protein (PLVAP*)*, which mediates vascular fenestration and promotes vascular leakiness, is highly upregulated in $Ndp^{y/-}$ retinas (18). Upregulation of PLVAP/MECA32 in retinal endothelial cells has also been shown for $Lrp5^{-/-}$ and $Tspan12^{-/-}$ mice (13). Furthermore, it was shown that upregulation of PLVAP indicates the loss of canonical Wnt signaling (19). The delayed outgrowth of the SRVP and the absence of deep sprouting could be caused either by defects in sprouting angiogenesis or by reduced proliferation of the SRVP. Sprouting angiogenesis is mediated by endothelial tip cells that guide the growing SRVP from the optic nerve head towards the retinal periphery along a VEGF gradient (20). Tip cell adjacent stalk cells divide ensuring proliferation and growth. Thus, an imbalance of tip and stalk cells could lead to both observed effects. The proper differentiation of tip and stalk cells is mediated by a balanced expression and interaction of Notch1 with its ligands Dll4 and Jagged1 (21-23). Dll4 is expressed in tip cells and induces Notch signaling in adjacent stalk cells. In contrast, Jagged1 is expressed in stalk cells impeding Notch signaling in adjacent tip cells. Disruption of Notch signaling have been shown to alter morphometric parameters such as the number of peripheral tip cell filopodia, vascular density and the number of vascular branch points. The outgrowth of the SRVP along the VEGF gradient involves MAPK signaling. VEGF, provided by astrocytes or retinal ganglion cells, binds a receptor complex consisting of VEGF receptor 2 (VEGFR2) and neuropilin 1 (Nrp1) activating downstream MAPK signaling. Loss of the cytoplasmatic Nrp1 domain ($Nrp1^{cyto\Delta/\Delta}$) or nestin specific knockout of VEGF ($VEGF_{NES\text{-}CRE}$) in mice causes artery/vein crossing in the SRVP of these mice. $VEGF_{NES\text{-}CRE}$ mice additionally show aberrant deep sprouting (24,25).

Here, we focused on defects during development of the SRVP in $Ndp^{y/-}$ mice. We quantified several vascular and angiogenic parameters and observed extensive vessel crossing within the SRVP which might be a Wnt-characteristic feature. We found reduced cell proliferation in the SRVP at the vascular front at P6 in $Ndp^{y/-}$ mice which may explain the delayed outgrowth of the SRVP. We also detected elevated mural cell coverage of the SRVP starting at P9, which is consistent with previously reported upregulation of *Tie1*, *Pdgfβ and Pdgfrβ*. Finally, we report for the first time endomucin positive supernumerary central filopodia of the SRVP in $Ndp^{y/-}$ retinas culminating at P9, the time point when the deep retinal vascular plexus (DRVP) normally would develop.

Results

Vascular development in Norrin knockout mice

The wildtype mouse retina is avascular at birth and outgrowth of the SRVP progresses from the center towards the periphery from P1 until P8. Because the outgrowth of the SRVP is incomplete and delayed in *Ndp*$^{y/-}$ mice (14), we hypothesized that there might be an imbalance between tip cell filopodia and/or adjacent stalk cell proliferation. We quantified the number of filopodia as well as the vascular density and number of branch points in the central plexus at the vascular front at P5 and P7 (Figure 1) (Supplementary Table 1). The number of filopodia was significantly increased and the vascular density (Figure 1 a, c, e, g, i, k) and the number of branch points (Figure 1 a, c, e, g, j, l) were significantly decreased at P5 and P7 in *Ndp*$^{y/-}$ mice. Moreover, filopodial protrusions in *Ndp*$^{y/-}$ mice are straighter and expand with a narrower angle than filopodia of wildtype littermates (Figure 1o) (Supplementary Table 2). In contrast to the increased number of filopodia, the vascular front in general appears to be less ramified with a reduced amount of long tip cell protrusions (Figure 1 b, f).

Comparison of vascular development in different mouse models

Available morphometric data from three Norrin-Wnt signaling knockout mice (*Fzd4* $^{-/-}$, *Lrp5* $^{-/-}$ and *Tspan12* $^{-/-}$), three Notch signaling knockout mice (*Dll4* $^{+/-}$, *Jag1*$^{i\Delta EC}$, *Nrarp*$^{-/-}$), *Ang2*$^{LZ/LZ}$ and Pax6 dependent hypoxia inducible factor 1 α (*HIF1α* $^{\Delta Pax6}$) knockout mice were compared (Table 1). The morphometric comparison of *Jag1*$^{i\Delta EC}$ with *Ndp*$^{y/-}$ mice was of special interest since Jag1 has been shown to be a canonical Wnt target gene in hair follicle cells comprising two LEF/TCF binding sites within its promoter region (26,27). We compared our morphometric data from Norrin KO mice with published morphometric data from *Jag1*$^{i\Delta EC}$ mice and recognized delayed and incomplete outgrowth of the SRVP, together with a reduced vascular density and a decreased number of branch points in *Jag1*$^{i\Delta EC}$ and *Ndp*$^{y/-}$ mice. In contrast to *Ndp*$^{y/-}$ mice, the number of tip cell filopodia was reduced in *Jag1*$^{i\Delta EC}$ mice. *Dll4* $^{+/-}$ mice have an increased number of filopodia, increased number of branchpoints and a denser vascular SRVP. Hence, the *Ndp*$^{y/-}$ phenotype of the SRVP displays as an intermingled picture, with a peripheral Jag1 loss of function but central Jag1 gain of function features. We asked the question whether or not Norrin is a negative regulator of Notch signaling. To answer this question, we examined the effect of Notch inhibition in *Ndp*$^{y/-}$ mice in order to see if this may rescue the abnormal vascular development. We quantified and compared morphometric parameters in Norrin knockout and wildtype mice after inhibition of Notch signaling by injection of the γ-secretase inhibitor DAPT (Figure 2). Administration of DAPT increased vascular density in wildtype and *Ndp*$^{y/-}$ mice (Figure 2a-e), while the number of filopodia only increased in wildtype but not in *Ndp*$^{y/-}$ retinas (Figure 2f-j) (Supplementary Table 3).

Retinal endothelial cell proliferation in Norrin deficient mice

To test the hypothesis if Norrin acts as a mitogen for cells in the SRVP, which would explain the reduced vascular density as well as the delayed and incomplete radial vascular outgrowth in *Ndp*$^{y/-}$ mice, we quantified central endothelial cell proliferation after systemic bromodeoxyuridine (BrdU) injection and found significantly reduced proliferation rates of isolectin B4 positive ECs from the SRVP in *Ndp*$^{y/-}$ mice at P6 (WT: ME±SD 101.71 ± 16.54 ; KO: ME±SD 52.17 ± 9.62; p-value: 1.8E-5) (Figure 3a, c). The only

exception from this observation is local hotspots of proliferation within bulky unorganized regions at the vascular front (Figure 3d). Additionally, we monitored the effect of Norrin on cell cycle progression in cell culture experiments by using an E2F transcription factor-mediated reporter assay (cell proliferation controlling transcription factor dependent luciferase reporter construct, reviewed in (28)). For this, we transiently transfected pE2F luciferase reporter constructs into HEK293T cells which extopically express the same amount of either human wildtype (p.=) or a pathogenic variant of Norrin containing the p.C95R mutation (Supplementary Figure 1), which has been associated with the classic picture of Norrie disease (29). HEK293T cells do not endogenously express Norrin, but were positive in RT-PCR for transcripts from *FZD4*, *LRP5* and *TSPAN12* (Supplementary Figure 1). Similarly to our BrdU data in $Ndp^{y/-}$ mice, we found almost six-fold increased cell cycle progression in cells that stably express human wildtype Norrin compared to cells that express the mutant Norrin isoform (Figure 3f, Supplementary Table 4).

Vascular remodeling in Norrin deficient mice

Despite the reduced vascular outgrowth of the superficial layer we occasionally noticed bulky vascular areas at the front of $Ndp^{y/-}$ mice, comprising three dimensional accumulations of endothelial cells (Figure 4d). To monitor vascular remodeling across the plexus, retinal whole-mounts were double stained for isolectin B4 (IB4) and collagen IV (ColIV). Collagen IV positive tubes lacking IB4 staining represent empty basement membrane sleeves at positions where blood vessels have regressed (30,31). We noticed that vascular remodeling was elevated in $Ndp^{y/-}$ mice at peripheral bulky vascular areas of the SRVP, but not in central areas (Figure 4c, white dots). Furthermore, we noticed vessel-crossing in $Ndp^{y/-}$ retinas. Vessels that morphologically resemble veins (venous character, VC) cross and grow below vessels that resemble arteries (arterial character, AC) between P7 and P21 (A/V crossing) (Figure 5, Supplementary Figure 3). ACs in Norrin knockout mice also interconnect less to the central plexus compared to wildtype and instead grow further into the periphery (Figure 6d). At P21, disorganized twisted and tangled blood vessels form above the superficial plexus resembling fibrosis (Supplementary Figure 3t, w). We hypothesized that A/V crossing could be caused by altered astrocyte-EC interaction and therefore co-stained astrocytes against PDGFRα and blood vessels with isolectin B4 (Supplementary Figure 2). We did not observe an altered astrocytic network in $Ndp^{y/-}$ retinas compared to wildtype and alignment between astrocytes and ECs was normal.

Mice lacking the Nrp1 cytoplasmatic domain or $VEGF_{NES\text{-}CRE}$ mice also show A/V crossing in the SRVP (24,25). This suggests that loss of MAPK signaling might cause this phenotype. Therefore we made use of our stably wildtype or p.C95R Norrin expressing HEK293T cell lines (Supplementary Figure 1) to monitor MAPK activity. We found a 1.9 fold increase of MAPK signaling in cells that express wildtype Norrin compared to those that expressed the mutant, disease-associated variant (Figure 5i, Supplementary Table 5).

Because of the above described, strong SRVP phenotype in $Ndp^{y/-}$ mice, it was crucial to examine if the VCs and ACs exhibit characteristic molecular features of the respective vessel types. Retinal flatmounts were stained either for endomucin or for smooth muscle actin at P7, P9, P12 and P21. In both, wildtype and $Ndp^{y/-}$ mice, endomucin stained veins and venous portions while staining of arteries and arterioles was less intense (Figure 7, Supplementary Figure 4) (32,33). Interestingly, the endomucin staining

revealed supernumerary thorn-like assembled central sprouts around veins and capillaries of *Ndp*$^{y/-}$ retinas (Figure 7d, e). In contrast, capillary sprouts were much less abundant and, if present, much shorter in wildtype mice. Staining for the arterial and mural cell (MC) marker α-smooth muscle actin (SMA) in wildtype mice specifically labeled arteries at P7, P9 and P12 as well as arteries and large veins at P21. In *Ndp*$^{y/-}$ retinas, arteries, veins and capillaries were covered with SMA positive cells at P9, P12 and P21. (Figure 7, Supplementary Figure 5). Thus, mural cell recruitment to the SRVP is abnormally increased in *Ndp*$^{y/-}$ retinas.

Discussion

Deficiency of Norrin is known to cause Norrie disease, a severe X-linked recessive human disease characterized by congenital blindness, progressive hearing loss and, in some patients, mental retardation. We made use of a mouse model which mimics the human disease in eye and ear and applied morphometric analyses, Notch-inhibition by DAPT administration, as well as cell proliferation assays to characterize the angiogenic processes in the retina. We provide evidence that Norrin is a mitogenic stimulus for cells in the SRVP. Consistently, wildtype Norrin promotes E2F transcription factor mediated cell cycle progression in a cell culture assay. Further, we identified endomucin as a marker for central filopodia, which were aligned in a thorn-like fashion at P9 in *Ndp*$^{y/-}$ mice. Finally, we found aberrant vascular SMA positive mural cell coverage of veins and capillaries from the SRVP in *Ndp*$^{y/-}$ mice which indicates abnormally increased mural cell recruitment of the SRVP from Norrin KO mice.

Norrin and Notch signaling are not directly linked

We examined features of the SRVP in *Ndp*$^{y/-}$ mice by quantifying and comparing morphometric parameters (Figures 1&3, Supplementary Tables 1, 2 & 3) with published data from different mouse models with retinal vascular phenotypes (Table 1). We did not quantify later stages than P7 since the outgrowth of the superficial plexus in wildtype mice ends soon after this stage of development.

We noticed that the outgrowth of the SRVP is delayed in all mouse models (Table 1), but incomplete vascular outgrowth was only observed in mutants with disrupted canonical Wnt signaling (*Ndp*$^{y/-}$, *Fzd4* $^{-/-}$ and *Lrp5* $^{-/-}$). Both, the deep and intermediate retinal vascular plexuses (DRVP, IRVP) are absent in mice with deficient Wnt signaling components (*Ndp*$^{y/-}$, *Fzd4* $^{-/-}$, *Lrp5* $^{-/-}$ and *Tspan12* $^{-/-}$) and in Ang2$^{LZ/LZ}$ mice, but not in Notch signaling deficient mice (*Dll4*$^{+/-}$ or *Jag1*$^{i\Delta EC}$). The intermediate plexus is absent in *HIF1α*$^{\Delta Pax6}$ mice while the deep plexus is present (Table 1). We hypothesized that the canonical Wnt target gene *Jag1* might link Norrin-Wnt and Notch signaling during development of the SRVP, since knocking out *Ndp* or *Jag1* leads to aberrant SRVP development. However, we found significant differences in morphometric parameters between *Ndp*$^{y/-}$ and *Jag1*$^{i\Delta EC}$ retinas, which is in conflict with this hypothesis. The number of filopodia was increased in *Ndp*$^{y/-}$ and reduced *Jag1*$^{i\Delta EC}$ mice. *Jag1*$^{i\Delta EC}$ retinas also do not display defects in deep vascular development (22) which is a characteristic feature in *Ndp*$^{y/-}$ retinas. All these phenotypic differences suggest that there is no direct link between Norrin-Wnt and Notch signaling via Jag1.

Inhibiting Notch signaling, through systemic DAPT administration led to an increased vascular density in *Ndp*$^{y/-}$ mice but it did not reduce the supernumerary filopodia. Furthermore, vascular density increased similarly in wildtype and *Ndp*$^{y/-}$ retinas after DAPT treatment, excluding a synergistic effect (Figure 3e). Accordingly, interaction effects were rejected by univariate analysis of variance (data not shown). Although the peripheral vascular network at the front is denser in DAPT-treated *Ndp*$^{y/-}$ mice (Figure 3d),

it still seems disorganized, three dimensional, and not planar. This implies that Notch inhibition can induce a peripheral hyper angiogenic response in *Ndp*$^{y/-}$ mice but not re-establish normal vascular development. The diameter of the peripheral blood vessels increased, which might be due to involvement of Dll4-Notch-signaling in A/V differentiation, leading to a more pronounced venous phenotype after DAPT injection and to an increase of vessel diameter (Figure 3a-d). The number of filopodia significantly increased in wildtype mice, but was unaltered in *Ndp*$^{y/-}$ retinas upon DAPT administration (Figure 3 g, I, j).

Vascular remodeling in Norrin deficient mice

We also found enhanced vascular proliferation (Figure 3) but also enhanced vascular regression/remodeling (Figure 4) at the vascular bulky front in *Ndp*$^{y/-}$ mice after BrdU injection and by co-staining of ColIV and isolectin B4. We interpret the vessel regression of *Ndp*$^{y/-}$ retinas as secondary effect which ensures a planar vascular plexus at positions where bulky vascular fronts were present before moving towards the periphery. Disorganized vascular fronts are also present in *Fzd4*$^{+/-}$, *Lrp5* $^{-/-}$ and *Tspan12*$^{-/-}$ retinas (12,13,34). Further, we observed extensive crossing of arteries and veins (A/V) in *Ndp*$^{y/-}$ retinas and we excluded an altered astrocytic scaffold to be the reason for these observations (Supplementary Figure 2).

Loss of Norrin signaling might alter MAPK signaling

A/V crossing is a feature of all Norrin-Wnt signaling deficient mice and also of VEGF-A$_{NES\text{-}CRE}$ and *Nrp1*$^{cyto\Delta/\Delta}$ mice (12,13,16,24). Also, the lack of the cytoplasmatic domain of Nrp1 (*Nrp1*$^{cyto\Delta/\Delta}$) or dosage dependent reduction of neuronal VEGF-A paracrine signaling (VEGF-A$_{NES\text{-}CRE}$) lead to A/V crossing (24,25). The receptor pair consisting of VEGFR2 and Nrp1 triggers VEGF mediated downstream MAPK signaling. Thus, the existence of A/V crossing in *Ndp*$^{y/-}$ retinas and in retinas from VEGF-A$_{NES\text{-}CRE}$ and *Nrp1*$^{cyto\Delta/\Delta}$ mice suggests that both pathways influence each other. Supporting this, Norrin stimulated cells have elevated MAPK signaling activity compared to cells stimulated with mutant Norrin (Figure 5i). Similarly, we previously reported MAPK signaling to be the major pathway influenced by Norrin signaling according to transcriptome analyses using microarray data from *Ndp*$^{y/-}$ retinas (18). Therefore it will be intriguing to investigate the putative link between Norrin-Wnt and VEGF/Nrp1/MAPK signaling.

Norrin stimulates mitogenic activity in retinal endothelial cells

Since loss of Norrin leads to delayed and incomplete outgrowth of the SRVP, we analyzed the mitogenic activity of Norrin in mouse retinas and in cell culture using systemic BrdU injection and reporter assays, respectively. The reduced proliferation of IB4 positive ECs from the SRVP in *Ndp*$^{y/-}$ retinas, as revealed after BrdU injection, indicates that Norrin might act as a mitogenic stimulus (Figure 3). Additionally, we monitored cell cycle progression by using the pE2F luciferase reporter construct. As expected, HEK293T cells, which endogenously express FZD4, LRP5 and TSPAN12 but not Norrin, and ectopically express human wildtype Norrin had an increased cell cycle progression compared to ectopically p.C95R mutant Norrin expressing cells (Figure 3f). Consistently, Ohlmann et al., 2010 observed, by using a BrdU ELISA, that Norrin efficiently stimulates proliferation of human retinal microvascular endothelial cells (HMECS) *in vitro* in a Wnt dependent manner. Our findings together with the BrdU ELISA suggest that Norrin might act as a mitogenic stimulus on microvascular/capillary endothelial cells of the SRVP (Figure 3c).

This also can explain the delayed outgrowth of the SRVP. A key to understand the complexity of the retinal vascular phenotype in *Ndp*$^{y/-}$ mice could be the differentiated view of events at the angiogenic front and within the central plexus. Transient peripheral phenomena like local hotspots of proliferation and remodeling, thickening of the vasculature and supernumerary filopodia could be interpreted as inability of vascular sprouts to escape the existing plexus. Hence, filopodia-projecting tip cells could be overrun by stalk cells, cluster, and form the observed bulky areas. The supposed explanation for the *Ndp*$^{y/-}$ superficial plexus phenotype is also supported by *in silico* models of vascular network formation. Travasso et al. recently found, utilizing a mathematical model of sprouting angiogenesis, that low tip cell motility leads to a sparsely ramified plexus and increased stalk cell proliferation (36). Due to the lack of long tip cell protrusions projecting into the avascular space ahead of the vascular front, also characteristic for *Ndp*$^{y/-}$ mice, stalk cells spend more angiogenic factors which decrease its concentrations and inhibits branching. The same study highlights that low overall EC proliferation also leads to reduced vessel ramification, corroborating our observations.

Veins and capillaries of *Ndp*$^{y/-}$ retinas possess supernumerary central filopodia

To investigate the properties of ACs and VCs, we stained retinal whole-mounts against endomucin and SMA.

The surface of veins and capillaries in *Ndp*$^{y/-}$ retinas was laced with endomucin positive filopodia instead of being smooth and covered with none or very few filopodia as in control mice. The abundance of central filopodia peaks around P9, exactly when deep vascular sprouting in wildtype mice occurs. Interestingly, deep sprouting exclusively originates from venous vessels and capillaries but not from arteries. Therefore it seems that veins and capillaries of the SRVP from *Ndp*$^{y/-}$ retinas are able to create misaligned central filopodia. However, these filopodia might not be functional, since *Ndp*$^{y/-}$ mice lack deep sprouting. It is also unclear which molecular mechanisms lead to those central supernumerary filopodia since published data focuses exclusively on the regulation of tip cell filopodia.

Veins and capillaries of *Ndp*$^{y/-}$ retinas are excessively covered by mural cells

Staining of retinal blood vessels for SMA revealed extensive MC coverage of veins and capillaries from P9 onwards. This coverage persists at least till P21. We previously reported upregulation of *PDGF*β and *PDGFR*β within the same timeframe (14). Interaction of all these genes regulates MC recruitment. Here, overexpression of *PDGFβ* and its receptor (*PDGFRβ*) could stimulate MC recruitment and the missing upregulation of *Ang1* on MCs might prevent restriction of MC recruitment. Considering this as the likely mechanism of the excessive MC recruitment, we believe that this might be a response to vessel leakiness caused by upregulation of *VEGF-A* and *PLVAP* (13,14,18) due to hypoxia. Currently, it is unclear if this extensive MC recruitment goes along with a gain of arterial character in the affected veins and venules. If so, the gain in arterial or loss of venous character could explain the disability to form the DRVP out of the SRVP from *Ndp*$^{y/-}$ retinas, since deep sprouts emerge exclusively from venous vessels and capillaries of the SRVP (38). The fact that we still can morphologically distinguish ACs and VCs and that we detected supernumerary endomucin positive central filopodia on veins, venules and capillaries, but not on arteries, argues against a complete loss of the venous character. However, the formation of uncoordinated central endomucin positive sprouts at P9 and the excessive MC recruitment of venous vessels may indicate at least a partial loss of venous identity of the respective endothelial cells with the consequence that central tip cells might develop, but being unable to induce proper deep sprouting.

The morphometric analysis together with results from the DAPT injections do not suggest a direct link between Norrin-Wnt and Notch signaling. Our results suggest that Norrin is a mitogenic stimulus for IB4 positive ECs of the SRVP which explains its delayed outgrowth in *Ndp* $^{y/-}$ mice. The A/V crossing occurs unlikely due to a disturbed astrocyte-EC interaction and it is unclear if the altered basal membrane of the SRVP contributes to this effect. We also found excessive MC coverage of veins, venules and capillaries in *Ndp*$^{y/-}$ retinas which might indicate a partial loss of venous identity but also contribute to the appearance of the altered basal lamina and possibly to the appearance of the thorn-like supernumerary central filopodia. Postnatal stages after P7 in mice mimic developmental stages from patients when hypoxia increases and leads to pathologic alterations of various retinal angiogenic maturation processes. Those data are crucial for the investigation of related diseases, like familial exudative vitreoretinopathy or Coats' disease, with a less severe phenotype than Norrie disease, which have a realistic chance for the development of treatment regimens.

Material and Methods

Animals

Generation of the *Ndp*$^{y/-}$ mouse line has been described elsewhere (4). The research was performed in accordance with the ARVO Statement for the Use of Animals in Ophthalmic and Vision Research and was approved by the Veterinary Office of the State of Zurich (Switzerland).

Immunohistochemical staining

Retinas for whole-mount immunohistochemistry were fixed in 4% paraformaldehyde for two hours or overnight at 4°C. After fixation, retinas were blocked using 1-10% normal goat or rabbit serum (VectorLabs) in PBST and subsequently incubated overnight with biotinylated isolectin B4 (1:200; VectorLabs). The following primary antibodies were diluted in 1-5% serum in PBST and incubated over

night: αSMA-CY3 (1:500; Sigma), Collagen IV (AbD serotec, 1:200), PDGFRα (R&D Systems, 1:500) and Endomucin (R&D Systems, 1:100). For secondary detection, Alexa Fluor streptavidin conjugates (Molecular Probes, 1:100) or anti-goat/rabbit Alexa Fluor-coupled secondary antibodies (Invitrogen, 1:500) were used. Retinas were washed five times with PBS, flat mounted and analyzed under bright-light illumination with a microscope (Axioplan 2, AxioCam HRc; Carl Zeiss) equipped with ApoTome (Carl Zeiss) or by confocal imaging using the CLSM Leica SP2 inverse microscope (Leica). The protocol from Pitulescu et al., 2010 was used to stain for proliferating endothelial cells (BrdU staining).

Image Processing

Image J 1.44p (NIH), Photoshop CS5 (Adobe) software were used for image processing. Overall image brightness was adjusted in a linear fashion on whole images if it was necessary to improve picture quality for prints. These adjustments did not influence interpretation and are in concert with suggestions for image processing in (39). Results shown were obtained by performing at least two different independent experiments including at least four mutant or control animals per stage.

Morphometric analysis of retinal flatmounts

Each morphometric parameter was determined by averaging over four non-overlapping images per retina (one retina used per animal) with a minimum of four animals per group. Vascular density was determined by measuring the endothelial coverage per 300x300 µm field at the vascular front. The number of branch points was determined by counting vessel branch points within 300x300 µm fields. The number of filopodia at the vascular front within 68x51 µm fields was counted and normalized to 100 µm length of vasculature. BrdU positive endothelial nuclei were counted in 424x317 µm fields at the vascular front and normalized to endothelial coverage within the same field (21).

***In vivo* Notch inhibition**

Notch signaling was inhibited by subcutaneous injection of 0.3 mg/g body weight N-[N-(3,5-Difluorophenacetyl-L-alanyl)]-S-phenylglycine t-butylester (DAPT, Merck) dissolved in 10% ethanol and 90% peanut oil. DAPT solution was injected twice at P5 and P6. Retinas were collected at P7. Control litters were injected with vehicle only. Seven litters were DAPT injected. Quantification of vascular density and number of filopodia in DAPT-treated versus untreated KO and WT mice were performed as described above (23).

Quantification of Norrin dependent proliferation and MAPK signaling *in vitro*

Stably wildtype or mutant C95R Norrin expressing HEK293T cells were used in these assays. Equal expression levels of wildtype and mutant Norrin were determined by western blot analysis (data not shown). To examine the proliferation rate or MAPK signaling activity, $8*10^4$ cells/well of a 24-well plate were seeded and incubated at 37°C/5% CO_2 overnight. Cells were transiently co-transfected with pE2F or pSRF firefly luciferase reporter and pRenilla constructs (SABiosciences) using the calcium precipitation method (40,41). Luciferase activity was measured using DualGlo-LuciferaseReporterAssaySystem (Promega). Firefly luciferase activity was normalized to co-transfected *Renilla* luciferase.

Statistical analysis

Statistical analysis was performed in SPSS 18.0 (IBM) using two-tailed unpaired Student's *t*-test. Quantitative data from DAPT-injection experiments were processed with univariate analysis of variance with two independent variables. Avoiding bias due to unequal sample sizes, the estimated marginal means where calculated instead of arithmetically means. *P*-values below α=0.05 were considered as significant.

Acknowledgments

We thank Britta Seebauer for contributing the immunostainings against α-SMA at P7. We also would like to thank Rui Benedito, Ralf Adams and Hiroyuki Yamamoto for giving practical advice and discussing this work as well as Wei Chi for donating the pFZD4 construct and He Xi and Bryan McDonalds for providing the pLRP5 construct. Conflict of Interest statement. None declared.

Funding

This work was supported by the Velux Foundation, Zurich, Switzerland and by the Swiss National Science Foundation [Grant number 31003A_122359], Bern, Switzerland.

References

1. Berger,W., Meindl,A., van de Pol,T.J., Cremers,F.P., Ropers,H.H., Doerner,C., Monaco,A., Bergen,A.A., Lebo,R., Warburg,M., . (1992) Isolation of a candidate gene for Norrie disease by positional cloning. *Nat. Genet.*, **1**, 199-203.

2. Berger,W., van de Pol,D., Warburg,M., Gal,A., Bleeker-Wagemakers,L., de,S.H., Meindl,A., Meitinger,T., Cremers,F., Ropers,H.H. (1992) Mutations in the candidate gene for Norrie disease. *Hum. Mol. Genet.*, **1**, 461-465.

3. Warburg,M. (1966) Norrie's disease. A congenital progressive oculo-acoustico-cerebral degeneration. *Acta Ophthalmol. (Copenh)*, Suppl-47.

4. Berger,W., van de Pol,D., Bachner,D., Oerlemans,F., Winkens,H., Hameister,H., Wieringa,B., Hendriks,W., Ropers,H.H. (1996) An animal model for Norrie disease (ND): gene targeting of the mouse ND gene. *Hum. Mol. Genet.*, **5**, 51-59.

5. Chen,Z.Y., Battinelli,E.M., Fielder,A., Bundey,S., Sims,K., Breakefield,X.O., Craig,I.W. (1993) A mutation in the Norrie disease gene (NDP) associated with X-linked familial exudative vitreoretinopathy. *Nat. Genet.*, **5**, 180-183.

6. Shastry,B.S., Hejtmancik,J.F., Trese,M.T. (1997) Identification of novel missense mutations in the Norrie disease gene associated with one X-linked and four sporadic cases of familial exudative vitreoretinopathy. *Hum. Mutat.*, **9**, 396-401.

7. Black,G.C., Perveen,R., Bonshek,R., Cahill,M., Clayton-Smith,J., Lloyd,I.C., McLeod,D. (1999) Coats' disease of the retina (unilateral retinal telangiectasis) caused by somatic mutation in the NDP gene: a role for norrin in retinal angiogenesis. *Hum. Mol. Genet.*, **8**, 2031-2035.

8. Shastry,B.S., Pendergast,S.D., Hartzer,M.K., Liu,X., Trese,M.T. (1997) Identification of missense mutations in the Norrie disease gene associated with advanced retinopathy of prematurity. *Arch. Ophthalmol.*, **115**, 651-655.

9. Ye,X., Wang,Y., Nathans,J. (2010) The Norrin/Frizzled4 signaling pathway in retinal vascular development and disease. *Trends Mol. Med.*.

10. Nikopoulos,K., Gilissen,C., Hoischen,A., van Nouhuys,C.E., Boonstra,F.N., Blokland,E.A., Arts,P., Wieskamp,N., Strom,T.M., Ayuso,C.*, et al.* (2010) Next-generation sequencing of a 40 Mb linkage interval reveals TSPAN12 mutations in patients with familial exudative vitreoretinopathy. *Am. J. Hum. Genet.*, **86**, 240-247.

11. Poulter,J.A., Ali,M., Gilmour,D.F., Rice,A., Kondo,H., Hayashi,K., Mackey,D.A., Kearns,L.S., Ruddle,J.B., Craig,J.E.*, et al.* (2010) Mutations in TSPAN12 cause autosomal-dominant familial exudative vitreoretinopathy. *Am. J. Hum. Genet.*, **86**, 248-253.

12. Xu,Q., Wang,Y., Dabdoub,A., Smallwood,P.M., Williams,J., Woods,C., Kelley,M.W., Jiang,L., Tasman,W., Zhang,K., Nathans,J. (2004) Vascular development in the retina and inner ear: control by Norrin and Frizzled-4, a high-affinity ligand-receptor pair. *Cell*, **116**, 883-895.

13. Junge,H.J., Yang,S., Burton,J.B., Paes,K., Shu,X., French,D.M., Costa,M., Rice,D.S., Ye,W. (2009) TSPAN12 regulates retinal vascular development by promoting Norrin- but not Wnt-induced FZD4/beta-catenin signaling. *Cell*, **139**, 299-311.

14. Luhmann,U.F., Lin,J., Acar,N., Lammel,S., Feil,S., Grimm,C., Seeliger,M.W., Hammes,H.P., Berger,W. (2005) Role of the Norrie disease pseudoglioma gene in sprouting angiogenesis during development of the retinal vasculature. *Invest Ophthalmol. Vis. Sci.*, **46**, 3372-3382.

15. Richter,M., Gottanka,J., May,C.A., Welge-Lussen,U., Berger,W., Lutjen-Drecoll,E. (1998) Retinal vasculature changes in Norrie disease mice. *Invest Ophthalmol. Vis. Sci.*, **39**, 2450-2457.

16. Xia,C.H., Yablonka-Reuveni,Z., Gong,X. (2010) LRP5 is required for vascular development in deeper layers of the retina. *PLoS. One.*, **5**, e11676.

17. Rehm,H.L., Zhang,D.S., Brown,M.C., Burgess,B., Halpin,C., Berger,W., Morton,C.C., Corey,D.P., Chen,Z.Y. (2002) Vascular defects and sensorineural deafness in a mouse model of Norrie disease. *J. Neurosci.*, **22**, 4286-4292.

18. Schafer,N.F., Luhmann,U.F., Feil,S., Berger,W. (2009) Differential gene expression in Ndph-knockout mice in retinal development. *Invest Ophthalmol. Vis. Sci.*, **50**, 906-916.

19. Liebner,S., Corada,M., Bangsow,T., Babbage,J., Taddei,A., Czupalla,C.J., Reis,M., Felici,A., Wolburg,H., Fruttiger,M.*, et al.* (2008) Wnt/beta-catenin signaling controls development of the blood-brain barrier. *J. Cell Biol.*, **183**, 409-417.

20. Gerhardt,H., Golding,M., Fruttiger,M., Ruhrberg,C., Lundkvist,A., Abramsson,A., Jeltsch,M., Mitchell,C., Alitalo,K., Shima,D., Betsholtz,C. (2003) VEGF guides angiogenic sprouting utilizing endothelial tip cell filopodia. *J. Cell Biol.*, **161**, 1163-1177.

21. Lobov,I.B., Renard,R.A., Papadopoulos,N., Gale,N.W., Thurston,G., Yancopoulos,G.D., Wiegand,S.J. (2007) Delta-like ligand 4 (Dll4) is induced by VEGF as a negative regulator of angiogenic sprouting. *Proc. Natl. Acad. Sci. U. S. A*, **104**, 3219-3224.

22. Benedito,R., Roca,C., Sorensen,I., Adams,S., Gossler,A., Fruttiger,M., Adams,R.H. (2009) The notch ligands Dll4 and Jagged1 have opposing effects on angiogenesis. *Cell*, **137**, 1124-1135.

23. Hellstrom,M., Phng,L.K., Hofmann,J.J., Wallgard,E., Coultas,L., Lindblom,P., Alva,J., Nilsson,A.K., Karlsson,L., Gaiano,N.*, et al.* (2007) Dll4 signalling through Notch1 regulates formation of tip cells during angiogenesis. *Nature*, **445**, 776-780.

24. Fantin,A., Schwarz,Q., Davidson,K., Normando,E.M., Denti,L., Ruhrberg,C. (2011) The cytoplasmic domain of neuropilin 1 is dispensable for angiogenesis, but promotes the spatial separation of retinal arteries and veins. *Development*, **138**, 4185-4191.

25. Haigh,J.J., Morelli,P.I., Gerhardt,H., Haigh,K., Tsien,J., Damert,A., Miquerol,L., Muhlner,U., Klein,R., Ferrara,N.*, et al.* (2003) Cortical and retinal defects caused by dosage-dependent reductions in VEGF-A paracrine signaling. *Dev. Biol.*, **262**, 225-241.

26. Katoh,M., Katoh,M. (2006) Notch ligand, JAG1, is evolutionarily conserved target of canonical WNT signaling pathway in progenitor cells. *Int. J. Mol. Med.*, **17**, 681-685.

27. Estrach,S., Ambler,C.A., Lo,C.C., Hozumi,K., Watt,F.M. (2006) Jagged 1 is a beta-catenin target gene required for ectopic hair follicle formation in adult epidermis. *Development*, **133**, 4427-4438.

28. Singh,S., Johnson,J., Chellappan,S. (2010) Small molecule regulators of Rb-E2F pathway as modulators of transcription. *Biochim. Biophys. Acta*, **1799**, 788-794.

29. Isashiki,Y., Ohba,N., Yanagita,T., Hokita,N., Doi,N., Nakagawa,M., Ozawa,M., Kuroda,N. (1995) Novel mutation at the initiation codon in the Norrie disease gene in two Japanese families. *Hum. Genet.*, **95**, 105-108.

30. Baluk,P., Morikawa,S., Haskell,A., Mancuso,M., McDonald,D.M. (2003) Abnormalities of basement membrane on blood vessels and endothelial sprouts in tumors. *Am. J. Pathol.*, **163**, 1801-1815.

31. Baffert,F., Le,T., Sennino,B., Thurston,G., Kuo,C.J., Hu-Lowe,D., McDonald,D.M. (2006) Cellular changes in normal blood capillaries undergoing regression after inhibition of VEGF signaling. *Am. J. Physiol Heart Circ. Physiol*, **290**, H547-H559.

32. Liu,C., Shao,Z.M., Zhang,L., Beatty,P., Sartippour,M., Lane,T., Livingston,E., Nguyen,M. (2001) Human endomucin is an endothelial marker. *Biochem. Biophys. Res. Commun.*, **288**, 129-136.

33. Samulowitz,U., Kuhn,A., Brachtendorf,G., Nawroth,R., Braun,A., Bankfalvi,A., Bocker,W., Vestweber,D. (2002) Human endomucin: distribution pattern, expression on high endothelial venules, and decoration with the MECA-79 epitope. *Am. J. Pathol.*, **160**, 1669-1681.

34. Chen,J., Stahl,A., Krah,N.M., Seaward,M.R., Dennison,R.J., Sapieha,P., Hua,J., Hatton,C.J., Juan,A.M., Aderman,C.M.*, et al.* (2011) Wnt signaling mediates pathological vascular growth in proliferative retinopathy. *Circulation*, **124**, 1871-1881.

35. Phng,L.K., Potente,M., Leslie,J.D., Babbage,J., Nyqvist,D., Lobov,I., Ondr,J.K., Rao,S., Lang,R.A., Thurston,G., Gerhardt,H. (2009) Nrarp coordinates endothelial Notch and Wnt signaling to control vessel density in angiogenesis. *Dev. Cell*, **16**, 70-82.

36. Travasso,R.D., Poire,E.C., Castro,M., Rodrguez-Manzaneque,J.C., Hernandez-Machado,A. (2011) Tumor angiogenesis and vascular patterning: a mathematical model. *PLoS. One.*, **6**, e19989.

37. Ohlmann,A., Seitz,R., Braunger,B., Seitz,D., Bosl,M.R., Tamm,E.R. (2010) Norrin promotes vascular regrowth after oxygen-induced retinal vessel loss and suppresses retinopathy in mice. *J. Neurosci.*, **30**, 183-193.

38. Fruttiger,M. (2007) Development of the retinal vasculature. *Angiogenesis.*, **10**, 77-88.

39. Rossner,M., Yamada,K.M. (2004) What's in a picture? The temptation of image manipulation. *J. Cell Biol.*, **166**, 11-15.

40. Jordan,M., Schallhorn,A., Wurm,F.M. (1996) Transfecting mammalian cells: optimization of critical parameters affecting calcium-phosphate precipitate formation. *Nucleic Acids Res.*, **24**, 596-601.

41. Jordan,M., Wurm,F. (2004) Transfection of adherent and suspended cells by calcium phosphate. *Methods*, **33**, 136-143.

42. Xia,C.H., Liu,H., Cheung,D., Wang,M., Cheng,C., Du,X., Chang,B., Beutler,B., Gong,X. (2008) A model for familial exudative vitreoretinopathy caused by LPR5 mutations. *Hum. Mol. Genet.*, **17**, 1605-1612.

43. Chen,J., Stahl,A., Krah,N.M., Seaward,M.R., Joyal,J.S., Juan,A.M., Hatton,C.J., Aderman,C.M., Dennison,R.J., Willett,K.L*., et al.* (2012) Retinal expression of wnt-pathway mediated genes in low-density lipoprotein receptor-related protein 5 (lrp5) knockout mice. *PLoS. One.*, **7**, e30203.

44. Gale,N.W., Thurston,G., Hackett,S.F., Renard,R., Wang,Q., McClain,J., Martin,C., Witte,C., Witte,M.H., Jackson,D*., et al.* (2002) Angiopoietin-2 is required for postnatal angiogenesis and lymphatic patterning, and only the latter role is rescued by Angiopoietin-1. *Dev. Cell*, **3**, 411-423.

45. Caprara,C., Thiersch,M., Lange,C., Joly,S., Samardzija,M., Grimm,C. (2011) HIF1A is essential for the development of the intermediate plexus of the retinal vasculature. *Invest Ophthalmol. Vis. Sci.*.

Figures and Tables

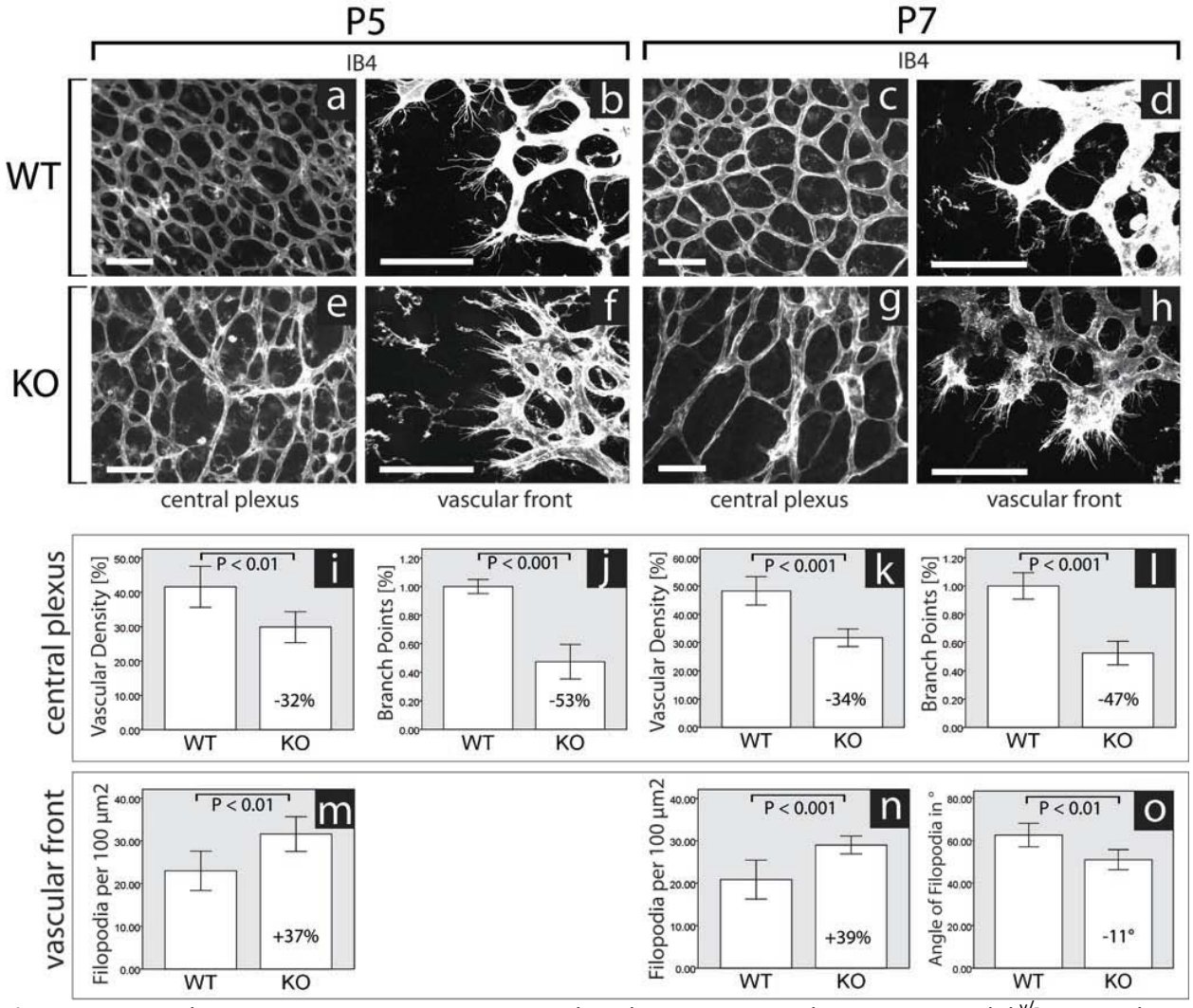

Figure 1. Morphometric parameters in norrin knockout versus wiltype mice. *Ndph*$^{y/-}$ mice show decreased vascular density, a decreased number of branch points but supernumerary filopodia, which are aligned in a more narrow angle compared to wildtype mice at P5 and P7. (a, e, c, g) Representative central retinal whole-mounts from wildtype (WT) and *Ndph*$^{y/-}$ (KO) retinas stained with isolectin B4 (IB4). (b, d, f, h) Representative peripheral retinal whole-mounts from WT and *Ndph*$^{y/-}$ retinas stained with IB4. Emerging filopodia are visible. Quantification of vascular density (i, k), number of branch points (j, l), number of filopodia (m, n) and angle of filopodia (o). Average and confidence intervals are shown. P-values below α=0.05 were considered statistically significant. Scale bars = 100 µm.

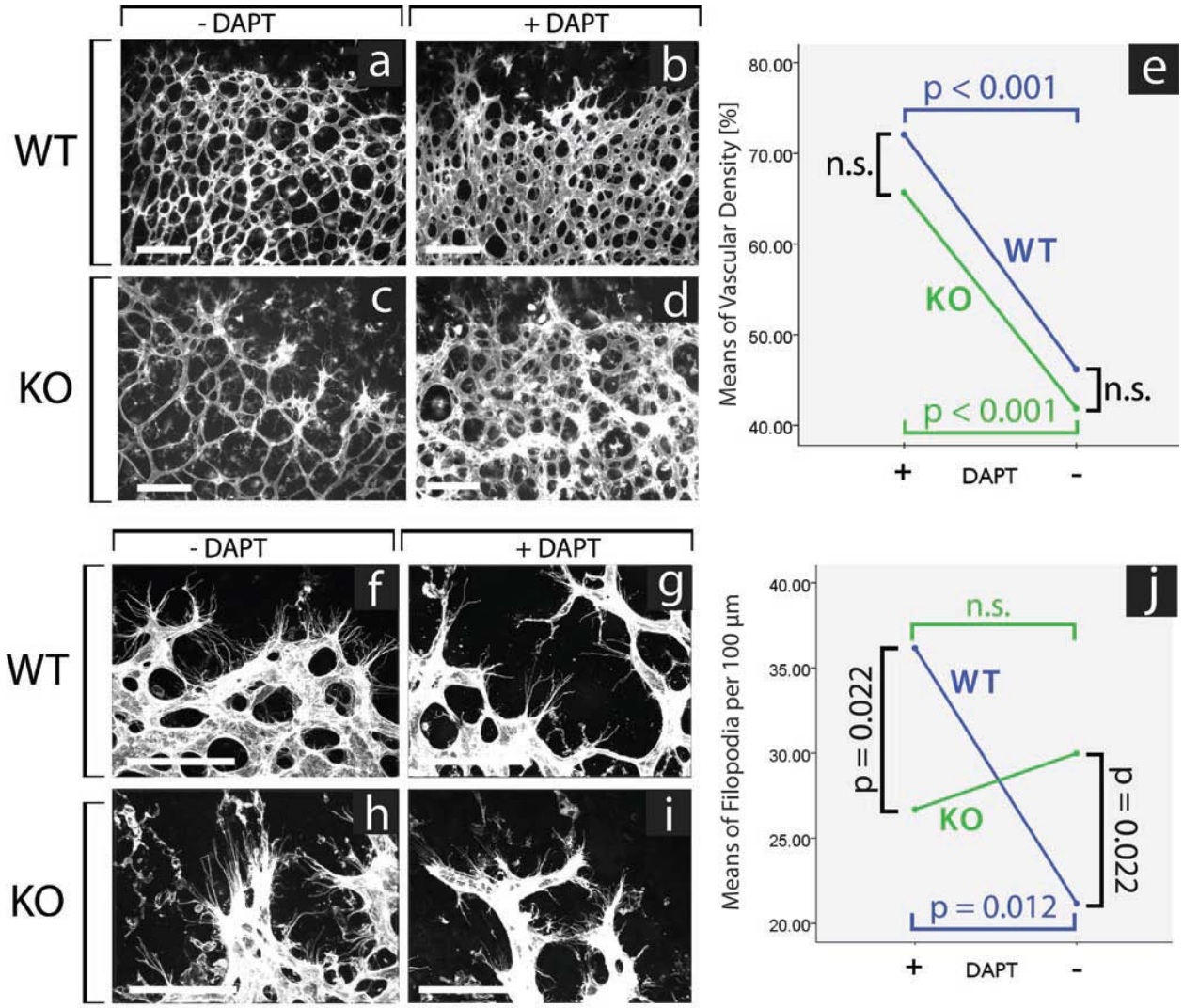

Figure 2. Effects of Notch signaling inhibition in wildtype and norrin knockout mice. Pharmacological administration of DAPT increases vascular density at the vascular front in wildtype and *Ndph*$^{y/-}$ mice. The number of filopodia only increases in wildtype but not in *Ndph*$^{y/-}$ mice upon DAPT treatment. (a, b, c, d) Representative retinal whole-mounts stained with isolectin B4 (IB4) 48h after DAPT injection in P7 wildtype (WT) and *Ndph*$^{y/-}$ (KO) animals. (e) Statistical analysis shows that peripheral vascular density increases in both genotypes upon DAPT treatment. (f, g, h, i) Representative retinal whole-mounts of isolectin B4 staining 48h after DAPT treatment of P7 wildtype (WT) and *Ndph*$^{y/-}$ (KO) animals. Filopodia at the vascular front are visible. (j) Statistical analysis shows that number of filopodia increases only after DAPT treatment in WT but not in *Ndph*$^{y/-}$ mice. P-values below α=0.05 were considered statistically significant. Scale bars = 100 µm.

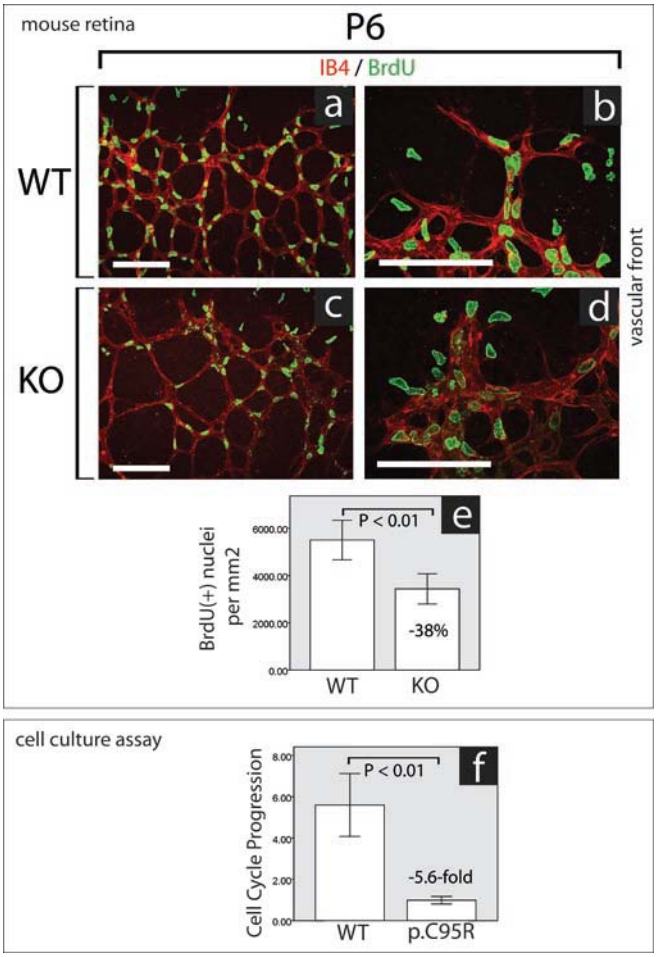

Figure 3. Decreased proliferation rate of endothelial cells in norrin knockout mice and reduced cell cycle progression due to a mutation (p.C95R) in human norrin. Overall proliferation is reduced in *Ndph*$^{y/-}$ mice at P6. Representative retinal whole-mounts of wildtype (WT) (a, b) and *Ndph*$^{y/-}$ mice (KO) (c, d) were stained for blood vessels with isolectin B4 (IB4, red) and for proliferating cells after BrdU incorporation (green). (d) Local hotspots of proliferation within thickened areas of the vascular front are occasionally seen in *Ndph*$^{y/-}$ mice and were excluded from quantification of proliferation. (e) Quantification of proliferating vascular endothelial cells after BrdU-incorporation revealed a reduced proliferation rate (-38%) in *Ndph*$^{y/-}$ mice. (f) Expression of wildtype norrin (WT) leads to 5.6-fold increase of proliferation rate in HEK293T cells compared to cells expressing a mutant (p.C95R) human norrin. RT = reverse transcriptase; Average and confidence intervals are shown. P-values below α=0.05 were considered statistically significant. Scale bars = 100 µm.

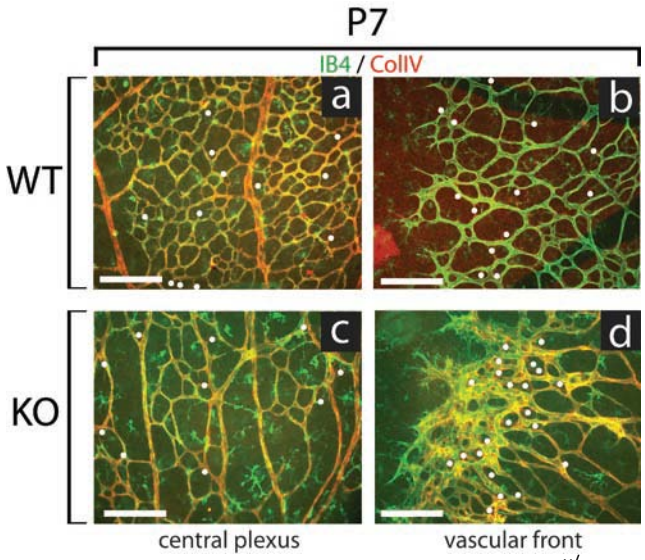

Figure 4. Massive vessel regression at the bulky vascular front in *Ndph*$^{y/-}$ mice at P7. Isolectin B4 (IB4, green) and collagenIV (ColIV, red) co-stained retinal whole-mounts from wildtype (WT) (a, b) and *Ndph*$^{y/-}$ mice (KO) (c, d). ColIV+, IB4- stainings represent empty membrane sleeves, where blood vessels have regressed (white dots). Regression was increased at the bulky vascular front in *Ndph*$^{y/-}$ retinas (d). Scale bars = 100 µm.

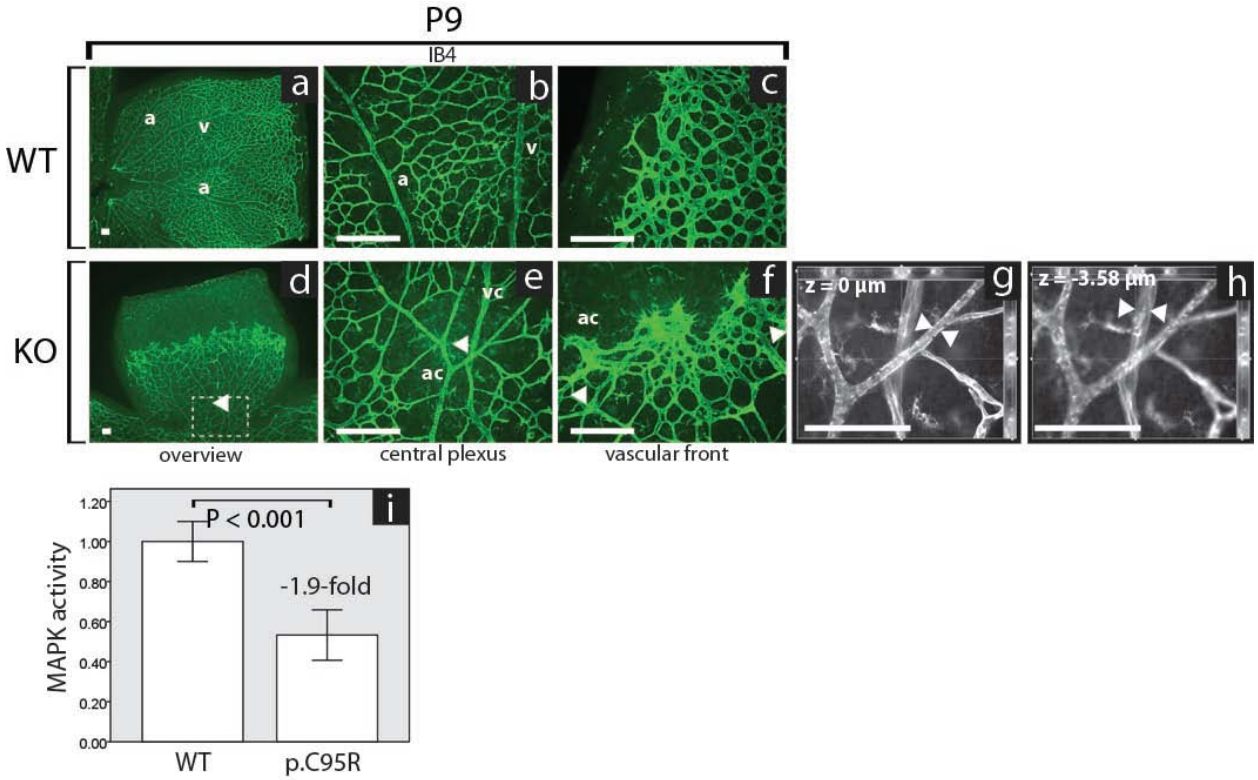

Figure 5. Blood vessel crossing in norrin knockout mice. Arteries and veins often cross each other in *Ndph*$^{y/-}$ retinas. Retinal wholemounts of wildtype (WT) (a-c) and *Ndph*$^{y/-}$ mice (KO) (d-h) were stained with isolectin B4 (IB4) to label blood vessels (green a-f, or grey g+h). We noticed abundant artery/vein crossings at the center (e, arrowheads) and periphery (f, arrowheads) of the superficial retinal vascular

plexus from *Ndph*$^{y/-}$ retinas. Note, that (e) represents the box indicated in (d). (g) and (h) are confocal images from the blood vessels marked in (e), focused on the upper artery (g), and on the lower vein (h). (i) Ectopic expression of wildtype norrin (WT) leads to 1.9-fold increase of MAPK signaling in HEK293T cells compared to cells expressing a mutant (p.C95R), disease-associated human norrin. The distance between both vessels is 3.58 µm. a = artery, ac = arterial character, v = vein, vc = venous character. Scale bars = 100 µm

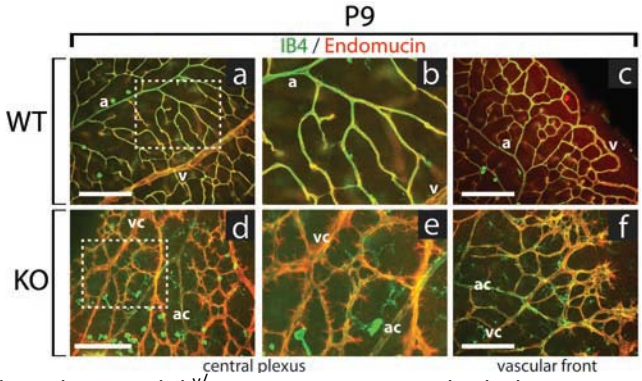

Figure 6. Large central filopodia in *Ndph*$^{y/-}$ mice at P9. Retinal whole-mounts from wildtype (WT) (a-c) and *Ndph*$^{y/-}$ mice (KO) (d-f) were co-stained with isolectin B4 (IB4, green) to label blood vessels and with endomucin (red) which preferentially stains veins, venous vessels and central filopodia. (b) represents box in (a), (e) represents box in (d). Endomucin staining revealed that vessels with a venous morphology (vc) but not with an arterial morphology (ac) are laced with supernumerary central filopodia. a = artery, v = vein. Scale bars = 100 µm.

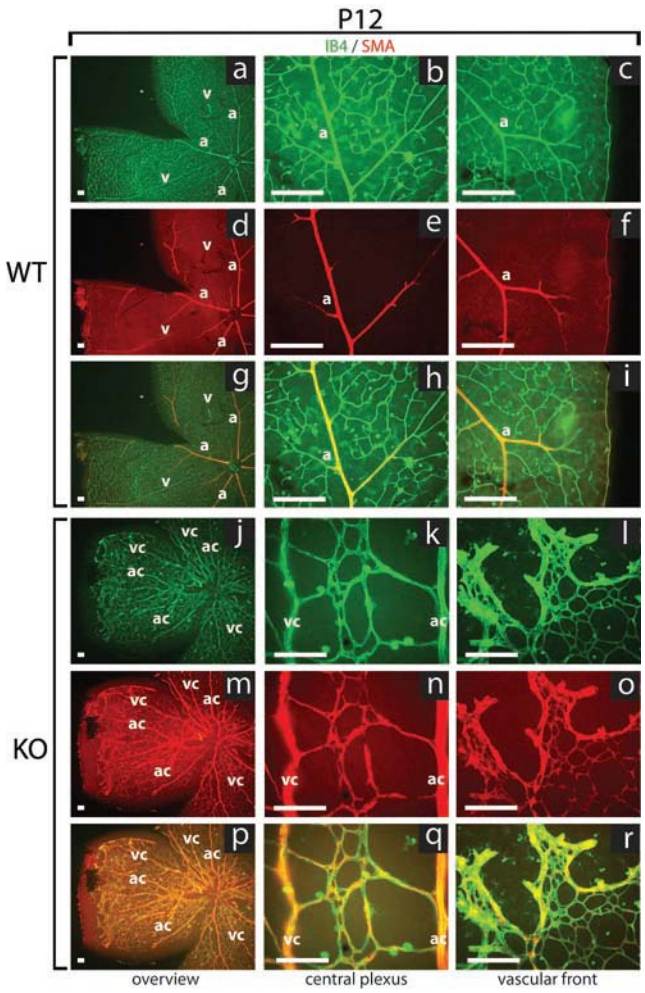

Figure 7. Retinal veins and capillaries are abundantly covered by vascular smooth muscle cells (vSMCs) in *Ndph*$^{y/-}$ mice at P12. Retinal whole-mounts were co-stained with isolectin B4 (IB4) to label blood vessels (green) and against smooth muscle actin (SMA) to label arteries covered by vSMCs (red). Only arteries were covered by vSMCs in wildtype (WT) retinas. In contrast, arteries, veins and capillaries were covered by vSMCs in *Ndph*$^{y/-}$ retinas (KO). a = artery, ac = arterial character, v = vein, vc = venous character. Scale bars = 100 µm.

Table 1: Morphometric data among mutant mice with comparable retinal vascular phenotype

	Ndp$^{y/-}$	*Fzd4*$^{-/-}$	*Lrp5*$^{-/-}$	*Tspan12*$^{-/-}$	*Dll4*$^{+/-}$	*Jag1*$^{i\Delta EC}$	*Nrarp*$^{-/-}$	*Ang*
Pathway affected	Canonical Wnt-signaling	Canonical Wnt- signaling	Canonical Wnt-signaling	Canonical Wnt-signaling	Notch-signaling	Notch-signaling; tamoxifen induced EC specific deletion	Notch, β-catenin/Lef1-dependent Wnt-signaling	Tie2 LZ =
Vascular outgrowth of SRVP	delayed and incomplete	delayed and incomplete	delayed and incomplete	delayed and incomplete	delayed	delayed (-44%)	delayed but complete	per ava
Vascular density of SRVP	reduced (-34%, P7)	not available	not available	reduced	increased (+58%*)	reduced (-32%, P6)	reduced at P5 but not different in adult	not
Number of branch points of SRVP	reduced (-47%, P7)	not available	not available	not available	increased (+96%*)	reduced (-65%, P6)	reduced at P5 but not different in adult	not
Number of filopodia of SRVP	increased (+39%, P7)	not available	not available	not avaiable	increased (sprouts increased +63%*)	reduced (-27%, P6)	not different at P5	not
A/V crossing in SRVP till P7	present	present	present	present	absent	absent	present	Not due qua
deep retinal vascular plexus	absent	absent	absent	absent	present	present	present	abs
intermediate retinal vascular plexi	absent	absent	absent	absent	present	present	present	abs
References	Luhmann et al., 2005 (14), this work	Xu et al., 2004 (12)	Xia et al., 2008 and 2010 (16,42,43)	Junge et al., 2009 (13)	Lobov et al., 2007 (21)	Benedito et al., 2009 (22)	Phng et al., 2009 (35)	Gal (44

*) % estimated from graph

Supplementary Figures

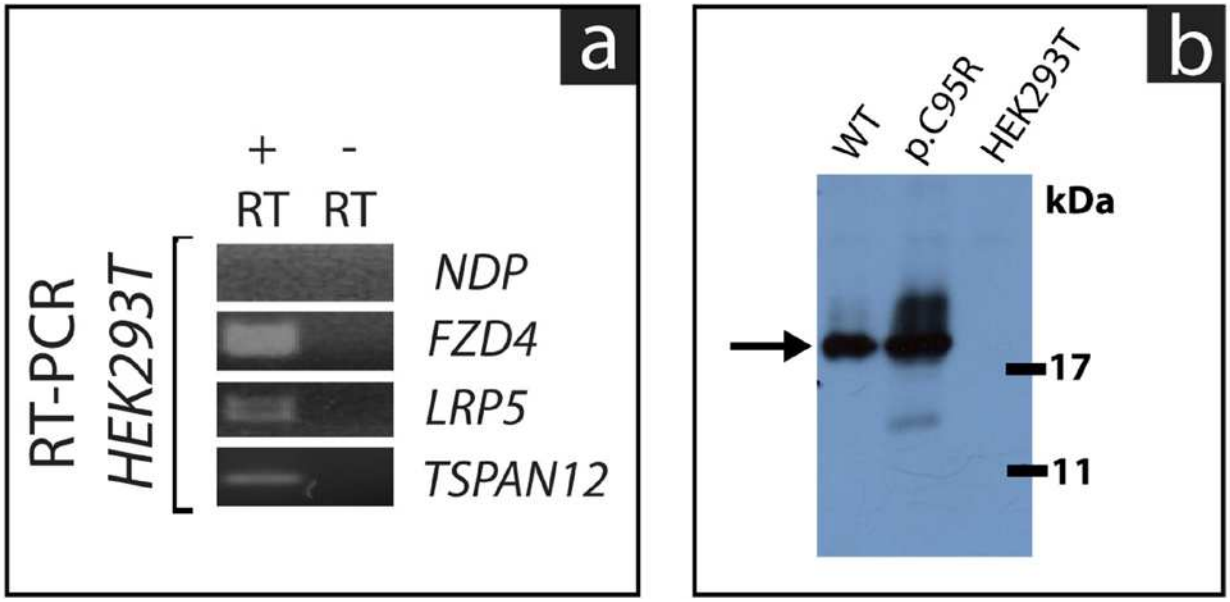

Supplementary Figure 1 HEK293T cells endogenously express Norrin receptors but no Norrin and the quantity of ectopic expression of wildtype and p.C95R Norrin in HEK293T cells is the same in both cell lines. (a) HEK293T cells used for this assay endogenously express FZD4, LRP5, TSPAN12 but no NDP. (b) Western blot analysis from protein extracts of HEK293T cells that express either wildtype (WT) or p.C95R (p.C95R) mutant Norrin or Mock (HEK293T). The arrow indicates the respective Norrin which appear slightly above 17 kDa.

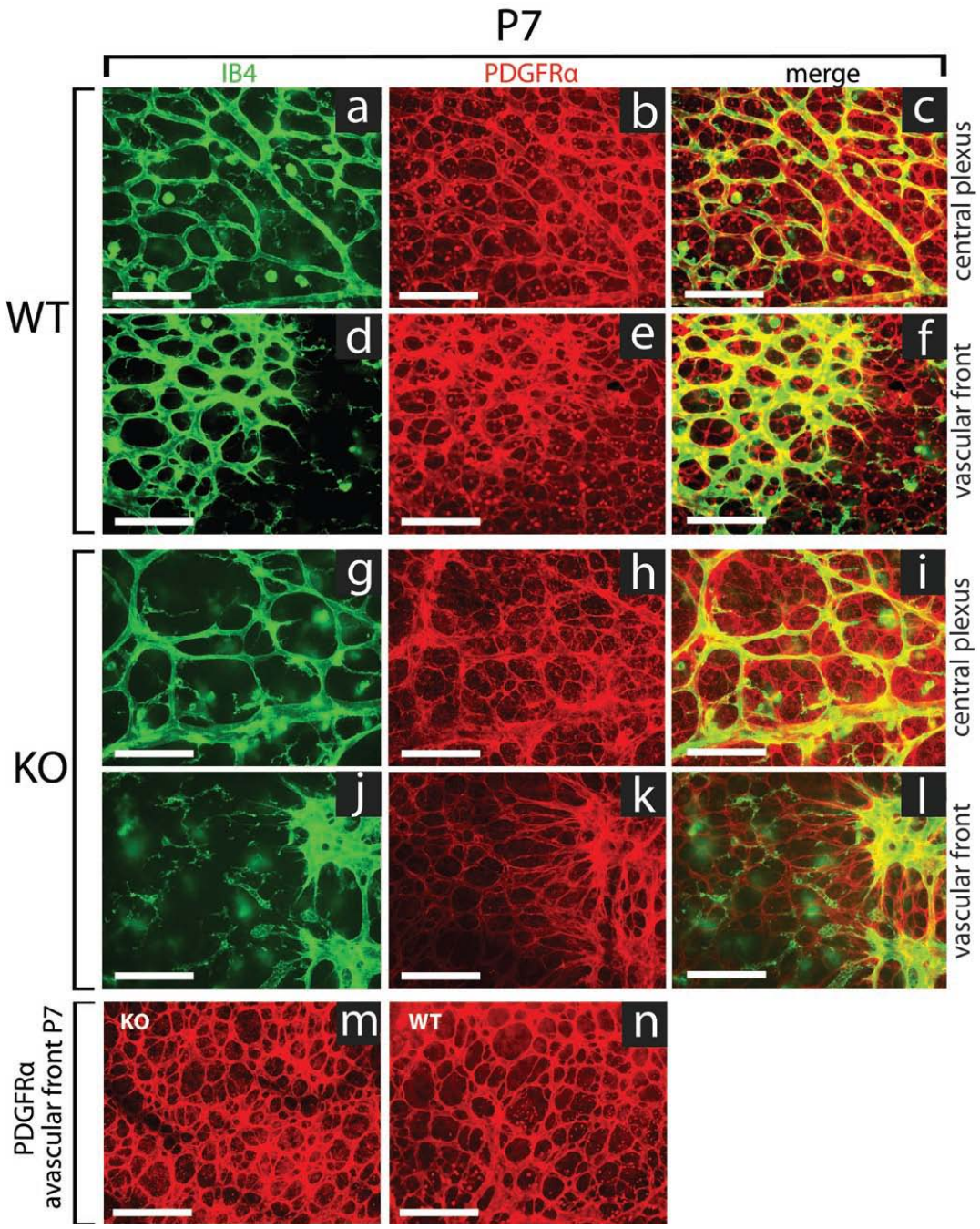

Supplementary Figure 2 Alignment of endothelial cells and astrocytes. Astrocyte/endothelial cell alignment is not altered in *Ndph*$^{y/-}$ mice at P7. Blood vessels of wildtype (WT) (a-f) and *Ndph*$^{y/-}$ retinas (KO) (g-l) were stained with isolectin B4 (IB4) to label blood vessels (green) and against PDGFRα to label astrocytes (red). Astrocytes align around the covering blood vessels in WT and KO mice. The density of the retinal astrocytic network at the avascular front is similar in *Ndph*$^{y/-}$ and wildtype retinas (m,n). Scale bar = 100 µm.

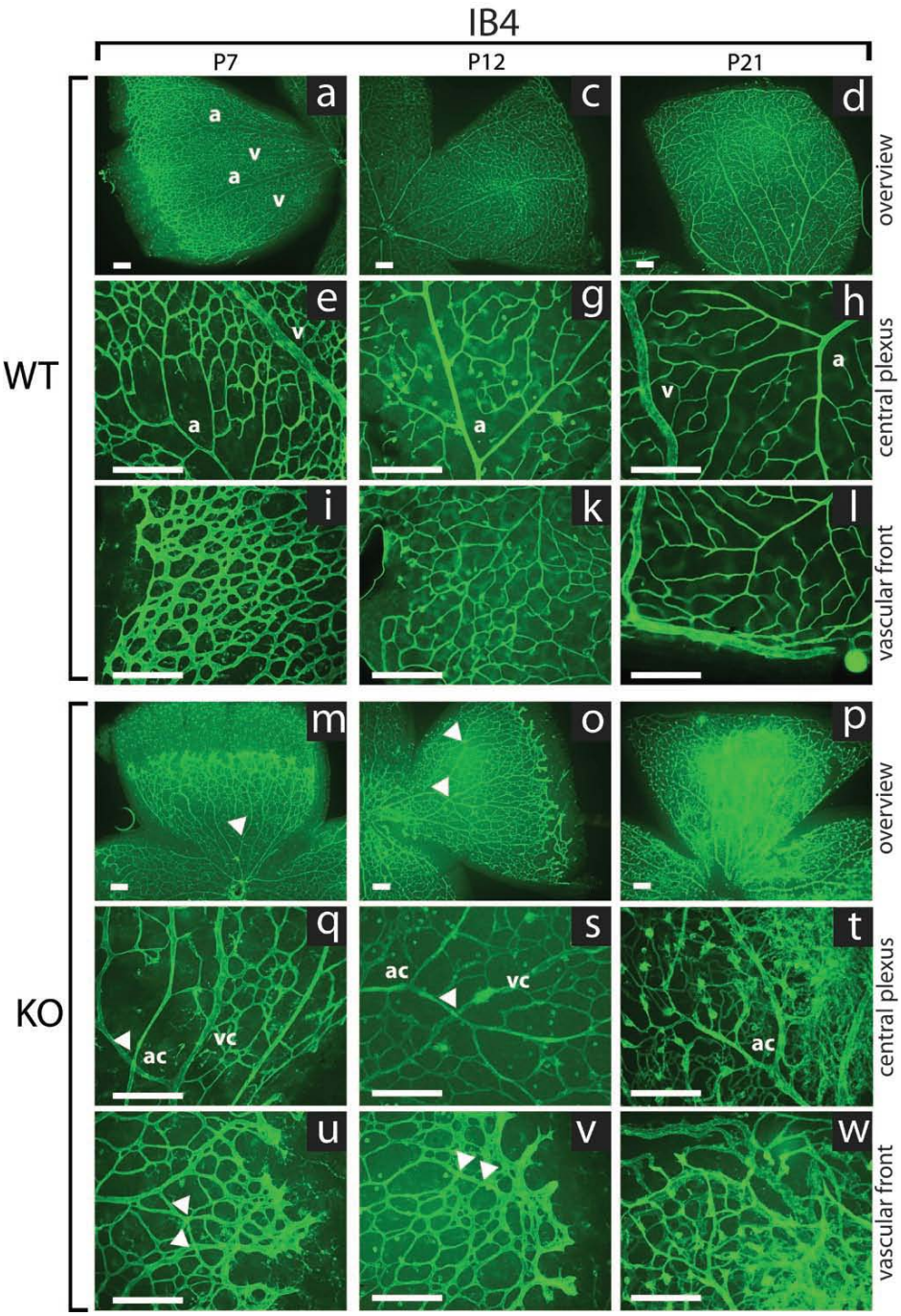

Supplementary Figure 3 Vessel crossing in norrin knockout mice. Arteries and veins often cross each other in *Ndph*$^{y/-}$ retinas between P7 and P21. Retinal wholemounts of wildtype (WT) (a-l) and *Ndph*$^{y/-}$ mice (KO) (m-w) were stained with isolectin B4 (IB4) to label blood vessels (green). We noticed abundant artery/vein crossing at the center (q, s, t) and in the periphery (u, v, w) of the superficial retinal vascular plexus from *Ndph*$^{y/-}$ retinas. a = artery, ac = arterial character, v = vein, vc = venous character. Scale bars = 100 µm

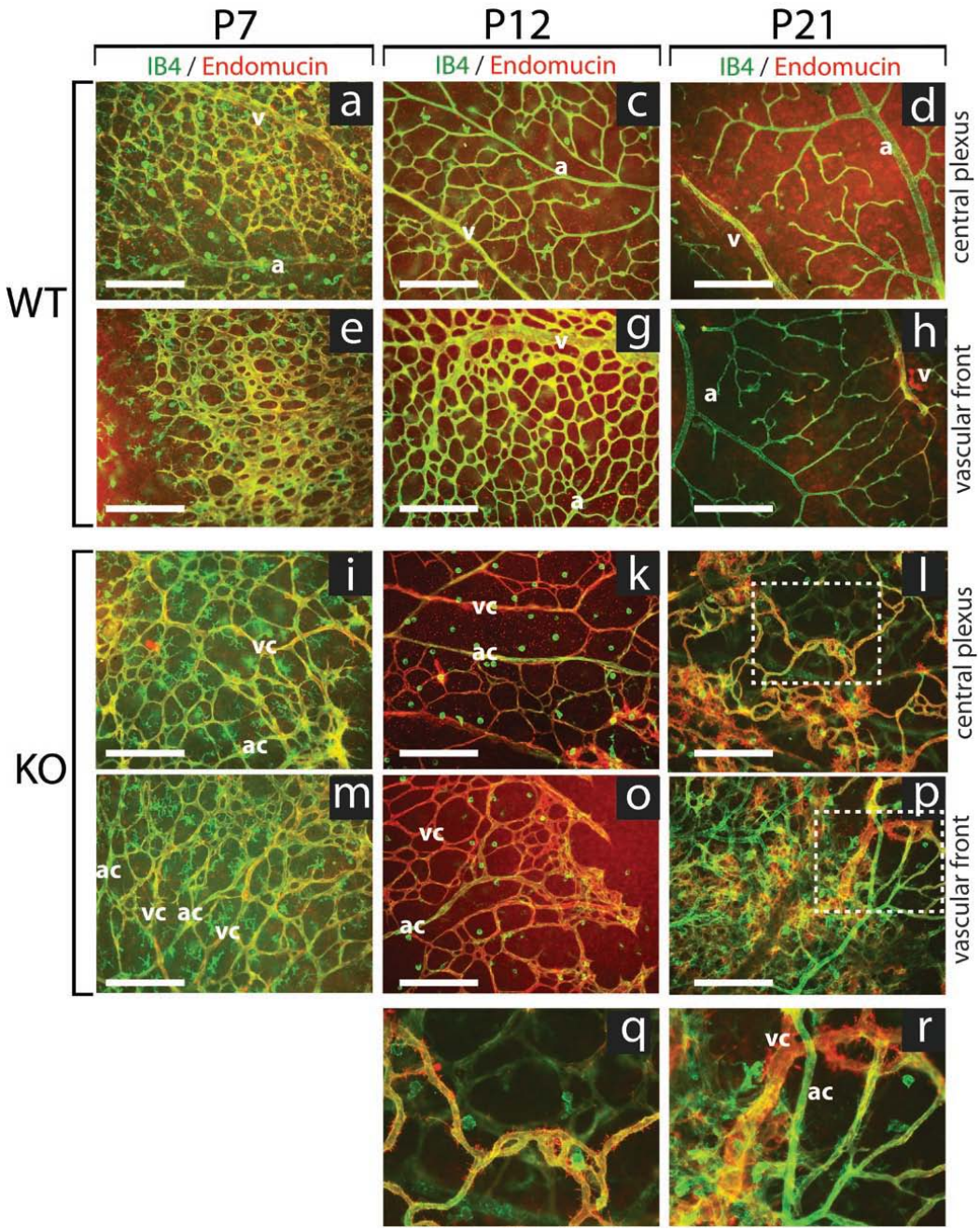

Supplementary Figure 4 *Ndph*$^{y/-}$ mice display small central filopodia at P12 and P21. Retinal flatmounts from wildtype (WT) (a-h) and *Ndph*$^{y/-}$ mice (KO) (i-r) were co-stained with isolectin B4 (IB4, green) to label blood vessels and with endomucin (red), which preferentially stained veins, venous vessels and central filopodia. (q) represents box in (l), (r) represents the box in (p). Endomucin staining revealed that vessels with venous character (vc) but no vessels with an arterial character (ac) are laced with small supernumerary central filopodia at P12 and P21 but not at P7. At P21, vessels grew above the superficial retinal vascular plexus resembling fibrosis. Fibrous vessels with vc but not ac were also laced with small filopodia (l, p, q, r). a = artery, v = vein. Scale bars = 100 µm.

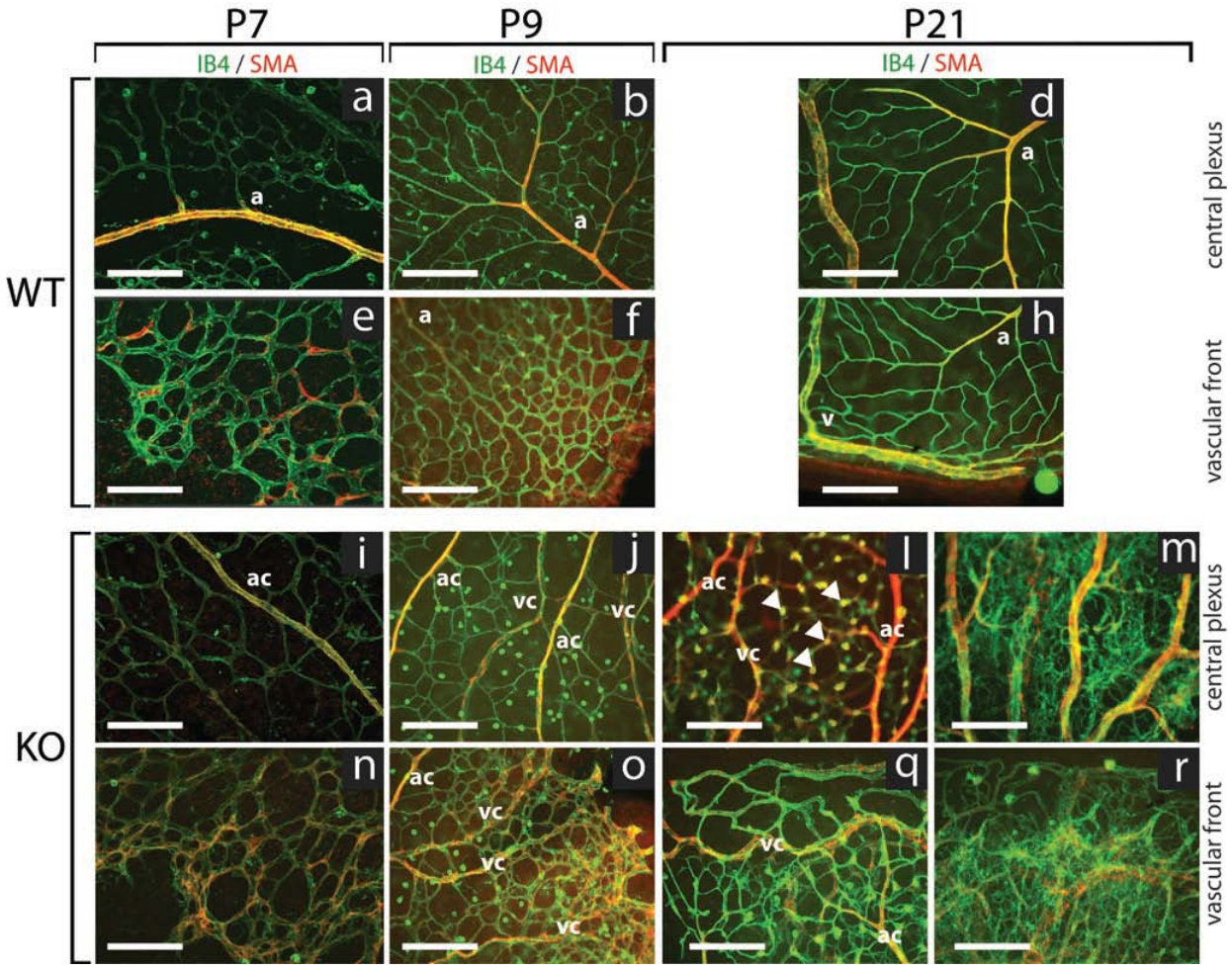

Supplementary Figure 5 Increased smooth muscle cell coverage of retinal veins and capillaries in norrin knockout mice. Retinal veins and capillaries are abundantly covered by vascular smooth muscle cells (vSMCs) in *Ndph*$^{y/-}$ mice at P9 and P21. Retinal flatmounts were co-stained with isolectin B4 (IB4) to label blood vessels (green) and against smooth muscle actin (SMA) to label arteries covered by vSMCs (red). Arteries were covered by vSMCs in wildtype (WT) retinas at P7 and P9 and arteries and veins at P21. In contrast, arteries, veins and capillaries were covered by vSMCs in *Ndph*$^{y/-}$ retinas (KO) between P9 and P21. At P21, some areas of the superficial retinal vascular plexus (SRVP) are abundantly overgrown with blood vessels resembling fibrosis (m, r). Overgrowth with blood vessels is prevented in other areas of the SRVP (l, q). These areas display drum stick like elongations that are entirely covered by vSMCs (arrowhead). a = artery, ac = arterial character, v = vein, vc = venous character. Scale bars = 100 µm.

Supplementary Table 1 Morphometric data from wildtype and *NDPh*$^{y/-}$ retinas

		wildtype retinas	NDPhy/- retinas
P5	Number of filopodia	23 ± 2 (n=5)	32 ± 5 (n=6; p-value = 0.001)
	Vascular density	42 ± 5 (n=5)	30 ± 4 (n=5; p-value = 0.002)
	Number of branchpoints	30 ± 1 (n=5)	14 ± 3 (n=5; p-value <0.0001)
P7	Number of filopodia	21 ± 3 (n=4)	29 ± 2 (n=7, p-value <0.0001)
	Vascular density	48 ± 4 (n=5)	32 ± 3 (n=7; p-value = 0.0006)
	Number of branchpoints	89 ± 7 (n=5)	47 ± 8 (n=7; p-value <0.0001)

average ± standard deviation are reported; n= number of retinas;

Supplementary Table 2 Filopodia angle

	wildtype retinas	*NDPh*$^{y/-}$ retinas
Filopodia angle in °	62.6 ± 29.0 (n=109)	51.0 ± 24.7 (n=109; p-value=0.002)

average ± standard deviation are reported; n= number of filopodia;

Supplementary Table 3 Quantification of morphometric parameters from wildtype and *NDPh*$^{y/-}$ mice after DAPT injection

Mean filopodia per 100 µm		WT +DAPT	WT -DAPT	KO +DAPT	KO -DAPT
	WT +DAPT	36 ± 7 (n=6)	p-value = 0.012	p-value =0.022	
	WT -DAPT		21 ± 3 (n=4)		p-value = 0.025
	KO +DAPT			27 ± 5 (n=6)	p-value = 0.279 (N.S.)
	KO -DAPT				30 ± 4 (n=4)
Mean vascular density		WT +DAPT	WT -DAPT	KO +DAPT	KO -DAPT
	WT +DAPT	72 ± 6 (n=6)	p-value = 0.00005	p-value = 0.149 (N.S.)	
	WT -DAPT		46 ± 5 (n=4)		p-value = 0.323 (N.S.)
	KO +DAPT			66 ± 8 (n=6)	p-value = 0.00067
	KO -DAPT				42 ± 5 (n=4)
Mean vascular length		WT +DAPT	WT -DAPT	KO +DAPT	KO -DAPT
	WT +DAPT	87 ± 3 (n=6)	p-value = 0.075 (N.S.)	p-value = 0.00002	
	WT -DAPT		83 ± 1 (n=4)		p-value = 0.00003
	KO +DAPT			70 ± 5 (n=6)	p-value = 0.022
	KO -DAPT				62 ± 2 (n=4)

average ± standard deviation are reported; n= number of retinas;

Supplementary Table 4 Cell cycle progression

	WT norrin	p.C95R norrin
Cell cycle progression	5.60 ± 0.61 (n=3)	0.99 ± 0.07 (n=3; p-value=0.00021)

average ± standard deviation are reported; n= number of technical replicas;

Supplementary Table 5 MAPK activity

	WT norrin	p.C95R norrin
MAPK activity	1.00 ± 0.040 (n=3)	0.53 ± 0.052 (n=3; p-value=0.00023)

average ± standard deviation are reported; n= number of technical replicas;